Contents lists available at SciOpen

Food Science and Human Wellness

journal homepage: https://www.sciopen.com/journal/2097-0765

China Food Publishing Co.

Combining network pharmacology, molecular docking, and experimental verification to investigate the anti-rheumatoid arthritis effect and mechanism of *Baeckea frutescens* leaves

Xueyang Guo[a], Mengyao Zhang[a], Haixia Cai[b], Xinyue Jiang[a], Siyuan Zhou[a], Wen Gong[a], Zijiao Wei[a], Weili Qiao[a], Beixi Jia[a,*]

[a] *Department of Pharmacognosy, School of Pharmaceutical Science, Zhengzhou University, Zhengzhou 450001, China*
[b] *Department of Pharmacy, Henan Provincial People's Hospital, Zhengzhou 450003, China*

ARTICLEINFO

Article history:
Received 31 October 2023
Received in revised form 24 November 2023
Accepted 16 January 2024

Keywords:
Baeckea frutescens leaves
Rheumatoid arthritis
5-Hydroxy-7-methoxy-2-isopropylchromone
Network pharmacology
Molecular docking

ABSTRACT

The aromatic *Baeckea frutescens* leaves (BFL) known as "Gang-Song-Cha" is a popular drink (Tea) in South China. To explore the healthcare value, a systematic and in-depth study on BFL alleviating rheumatoid arthritis (RA) was carried out by integrating network pharmacology, molecular docking, and experimental verification. The efficacy was first evaluated, and the BFL extract could ameliorate RA by inhibiting articular swelling, lowering immune organ index, improving the ankle pathologies, and regulating serum levels of tumor necrosis factor α (TNF-α), interleukin (IL)-6, and IL-10 in CIA rats. Then the anti-RA mechanism of BFL was investigated by leveraging the high-content and active component 5-hydroxy-7-methoxy-2-isopropylchromone (Chro), and the potential signaling pathway and related target proteins for Chro acting on RA were analyzed by Kyoto Encyclopedia of Genes and Genomes (KEGG) enrichment and docking simulation. Finally, the experimental validations were conducted on rheumatoid arthritis fibroblast-like synoviocytes (RA-FLS), and compound Chro could inhibit cell invasion and migration, block cell cycle at G2/M phase and induce apoptosis, and reduce the secretion of inflammatory cytokines by suppressing the PI3K-Akt pathway. These results provided pharmacological basis for the folk usage of "Gang-Song-Cha" for intervening RA.

© 2025 Beijing Academy of Food Sciences. Publishing services by Tsinghua University Press.
This is an open access article under the CC BY-NC-ND license
(http://creativecommons.org/licenses/by-nc-nd/4.0/).

1. Introduction

Baeckea frutescens is an aromatic plant of Myrtaceae, distributing from Australia to Southeast Asia[1-2]. In addition to being an ornamental plant, it is also an important raw material for the food and spice industry. In recent years, the delicate leaves of *B. frutescens* resembling pine needles, have been collected for tea known as "Gang-Song-Cha" in the southern part of China, and its healthcare value in the functional food field is being explored.

Modern researches have revealed the presence of essential oil[3-4], phloroglucinols[5-7], chromones[8-9], and flavonoids[10-12] in *B. frutescens* leaves (BFL), with the biological activities of antioxidation[13], anti-bacterial[14-16], anti-inflammation[17-20], and anti-tumor[6,21-22]. Acute oral toxicity investigations revealed that there were no mortalities and no adverse effects were observed in the methanol extract[23], alcohol extract[24] and water extract[25], suggesting BFL was safe for human consumptions. Its folk applications mainly focus on alleviating various inflammatory related diseases, such as high fever, icteric hepatitis, gastroenteritis, cystitis, and rheumatoid arthritis (RA), but there is a lack of systematic and in-depth study.

RA is a chronic, inflammatory, and autoimmune disease, which is prone to persist repeatedly and difficult to cure[26]. Primary clinical

* Corresponding author at: Department of Pharmacognosy, School of Pharmaceutical Science, Zhengzhou University, Zhengzhou 450001, China.
E-mail address: jiabeixi_2003_123@163.com (B.X. Jia)
Peer review under responsibility of Beijing Academy of Food Sciences.

SciOpen Publishing services by Tsinghua University Press

http://doi.org/10.26599/FSHW.2024.9250166
2213-4530/©2025 Beijing Academy of Food Sciences. Publishing services by Tsinghua University Press. This is an open access article under the CC BY-NC-ND license (http://creativecommons.org/licenses/by-nc-nd/4.0/).

drugs (mainly synthesized chemicals) have certain therapeutic effects on improving RA symptoms, but are not conducive for long-term medication due to adverse reactions[27]. Natural plants or compounds play unique roles in intervening RA, with advantages of integrated regulations of multi-targets and multi-pathways, and lower toxicity and cost[28-30]. It was reported that compound baeckein E (BF-2) from the plant *B. frutescens*, as an EP4 antagonist, could significantly inhibit the toe swelling of collagen-induced arthritis (CIA) mice, and relieve the degradation of articular cartilage matrix and inflammatory cell infiltration within the dose range of 25−100 mg/kg[31].

Based on preliminary experiments and current anti-RA drug research and development platform in our laboratory, an integration of network pharmacology, molecular docking, and experimental verifications *in vivo* and *in vitro* was designed to explore the anti-RA effect and mechanism of BFL. The results revealed evidenced pharmacological information for BFL alleviating RA, which provided a theoretical basis for the folk functional usage of "Gang-Song-Cha" for health food purpose.

2. Materials and methods

2.1 Reagents and chemicals

Bovine type II collagen (No. 20022) and incomplete Freund's adjuvant (No. 7002) were purchased from Chondrex (Redmond, WA, USA). Enzyme-linked immunosorbent assay (ELISA) kits, including rat tumor necrosis factor α (TNF-α) (No. JL13202), interleukin 6 (IL-6) (No. JL20896), IL-10 (No. JL13427) were obtained from Jianglai Biotechnology Co., Ltd. (Shanghai, China). Cell Counting Kit-8 (CCK-8) was bought from Jiancheng Bioenginering Institute (Nanjing, China). Dulbecco's modified eagle's medium (DMEM), phosphate buffered saline (PBS), Tris, glycine, 4% paraformaldehyde and TBST were provided by Beijing Solarbio Science and Technology Co., Ltd. (Beijing, China). Annexin V-fluorescein 5-isothiocyanate (FITC)/ propidium iodide (PI) double staining kit was taken from Jiangsu KeyGEN BioTECH Co., Ltd. (Nanjing, China). Apoptosis detection kit was produced by Bestbio Biotechnology Co., Ltd. (Shanghai, China). Crystal violet (1%), DEPC ddH_2O, ethidium bromide solution, and BCA protein concentration assay kit were obtained from Leagene Biotechnology Co., Ltd. (Beijing, China). IL-6 (No. EK106HS), IL-8 (No. EK108HS), IL-1β (No. EK101BHS), and matrix metalloproteinase 3 (MMP-3) (No. EK1M03) ELISA kits were obtained from MultiSciences Biotech Co., Ltd. (Hangzhou, China). RNA simple total RNA kit (No. CW0581), reverse transcription kit (No. 2569), fluorescence quantitative kit (No. CW0659), and Tris acetate-ethylene diamine tetraacetic acid (EDTA) buffer (50 ×) were bought from Jiangsu Cowin Biotech Co., Ltd. (Taizhou, China). Nonpyrogenic-RNase/Dnase-free pipet tips, Matrigel, and microtubes were provided by Corning-Axygen (NY, USA). Primers used for polymerase chain reaction (PCR) were designed by Sangon Biotech Co., Ltd. (Shanghai, China). Anti-phosphatidylinositol 3-kinase (PI3K) (No. 4257), anti-p-PI3K (No. 4228), anti-protein kinase B (AKT) (No. 4691), anti-p-AKT (No. 4060), anti-p-p65 (No. 3033), anti-3-phosphoinositide-dependent protein kinase 1 (PDK1) (No. 3062), anti-Cyclin B1 No. 12231), anti-myeloid cell leukemia 1 (Mcl-1) (No. 5453), anti-Bcl-2 (No. 4223), anti-cyclin dependent kinase 1 (CDK1) (No. 77055), anti-CDK2 (No. 18048), anti-cleaved Caspase 3 (No. 9664) primary antibodies were purchased from Cell Signaling Technology, Inc. (MA, USA). Anti-p65 (No. AF5006) primary antibody was bought from Affinity Biosciences (Changzhou, China). Anti-*β*-actin (No. 20536-1-AP) primary antibody and HRP-conjugated affinipure goat anti-rabbit IgG (H + L) secondary antibody (No. SA00001) were obtained from Proteintech Group, Inc. (Wuhan, China). Human TNF-α (No. 96-300-01A) was produced by PeproTech (NJ, USA). Ladder DNA Marker (100 bp) (No. SM0241) and PageRuler Prestained Protein Ladder (No. 26616) were taken from Thermo Fisher Scientific (MA, USA). Sodium dodecyl sulfate-polyacrylamide gel electrophoresis (SDS-PAGE) gel kit (No. WB-0201) was provided by Beijing Dingguo Changsheng Biotechnology Co., Ltd. (Beijing, China). RIPA (No. PC101) produced by Epizyme Biotech (Shanghai, China) was selected. Antibody dilution buffer (No. P0256) and high-sensitivity ECL chemiluminescence kit (No. P0018AS-2) were bought from Beyotime Biotechnology (Shanghai, China). Polyvinylidene fluoride (PVDF) membrane was provided by Millipore Corporation (MA, USA).

Tripterygium polyglycosides tablets (TPT) (No. 20181108) was produced by Fudan Forward Pharmaceutical Co., Ltd. (Shanghai, China). Methotrexate (MTX) (No. R000499) was purchased from Shanghai Yuanye Biotechnology Co., Ltd. (Shanghai, China). 740 Y-P (No. HY-P0175) was bought from MedChemExpress (NJ, USA). Compound myricetin-3-*O*-*α*-*L*-rhamnopyranoside (Myricitrine) and 5-hydroxy-7-methoxy-2-isopropylchromone (Chro) were isolated from *B. frutescens* in our laboratory. The chemical structures were determined by electrospray ionization-mass spectrometry (ESI-MS), ^{1}H- and ^{13}C-NMR, and the purity was more than 98% through normalization of the peak area detected by high-performance liquid chromatography-diode array detection (HPLC-DAD).

2.2 Plant material and sample preparation

The leaves of *B. frutescens* collected from Guangxi Province, China, were authenticated by Professor Cheng-Xue Pan (Department of Pharmacognosy, School of Pharmaceutical Science, Zhengzhou University, Zhengzhou, China), and the voucher specimen (No. GS-L-001) was deposited in above institution. The dried leaves (1.0 kg) were extracted with 95% ethanol for three times under reflux. The total extracting solutions were evaporated to dryness at 50 °C under reduced pressure. And the residue (89.0 g) was stored in a dryer for subsequent testing.

2.3 Pharmacodynamic evaluation in vivo

2.3.1 Animals

The female SD rats (weight 180−200 g) were provided by the Henan Experimental Animal Center, Zhengzhou, China, and the certificate number is SYXK (Yu) 2018-0004, and maintained under standard laboratory conditions. All the experimental procedures were carried out following the Care and Use of Laboratory Animals (the National Institutes of Health), and approved by the Ethical Committee of Zhengzhou University (No. yxyllsc20220069).

2.3.2 CIA induction and treatment

Bovine type II collagen was emulsified with incomplete Freund's adjuvant (IFA) in 1:1 (*V*/*V*) proportion. The IFA emulsion (0.25 mL)

was intradermally injected into the tail bases of rats on day 0 to induce CIA, followed by a booster injection on day 7 for a second immunization. On day 24, the immunized CIA rats were randomly divided into 5 groups (n = 8), and were intragastrically administered one of the following: 0.5% carboxymethylcellulose (CMC)-Na solution (the model group), 10 mg/(kg·day) TPT (the positive control group), and 1.5, 3.0, 6.0 g/(kg·day) BFL (the low-, medium-, high-dose group, namely BF-L/M/H, respectively) for 20 days. Rats in the normal control group without CIA induction, were treated with the same amount of 0.5% CMC-Na in an identical manner as those in experimental group.

2.3.3 Measurement of the toe swelling and arthritis score of rats

From day 0, the general situation of diet, hair color, mental state, activity, body weight, toe swelling, and arthritis of rats were recorded every 4 days. The thickness of left and right hind feet of the rats was measured by an electronic vernier caliper (Radio shack, TX, USA), and the difference before and after inflammation was taken as the degree of toe swelling. The arthritis severity was assessed by a scoring system of the reported scale 0–4[32], and the arthritis score more than 4 indicated a successful CIA model, while the maximum score value for each rat was 16.

2.3.4 Thymus and spleen indices assays

On day 44, the rats were sacrificed via anesthesia (1% pentobarbital sodium, 40 mg/kg, i.p.). The thymus and spleen were removed and weighed in time. And the index of thymus and spleen were expressed as the ratio of thymus and spleen wet weight versus body weight (mg/g).

2.3.5 X-ray imaging and histopathological analysis

After the rats were anesthetized, X-ray imaging (Carestream Health, Toronto, Canada) was performed on all rats to evaluate the joint spaces and the degree of bone erosion. After the rats were sacrificed, the synovial tissue of ankle and knee joints were taken out immediately and fixed with 4% paraformaldehyde and decalcified with 10% EDTA. Subsequently, the specimen was embedded in paraffin, sectioned into thick slices, and stained with hematoxylin & eosin (H&E). The histological structure and pathological changes of the joints were observed by light microscope.

2.3.6 Detection of TNF-α, IL-6, and IL-10 in rat serum

Twelve hours after the last administration, rats were anesthetized, and the blood was collected from the abdominal aorta and centrifuged at 3 000 r/min for 15 min at 4 °C to collect upper serum. The levels of TNF-α, IL-6 and IL-10 in serum were detected by ELISA kits.

2.4 HPLC analysis

The dried BFL extract (30 mg) was dissolved in methanol and marked up to 10 mL, and the solution was filtrated through a 0.45 μm syringe filter before HPLC analysis. The detection conditons and parameters previously used in our lab were refered here[33].

2.5 Anti-inflammatory assay

The RAW264.7 mouse macrophage cell line was obtained from Cell Bank of the Chinese Academy of Sciences (Shanghai, China), and cultured in DMEM supplemented with 10% (V/V) fetal bovine serum (FBS) (Biological Industries, Israel), penicillin (100 U/mL) and streptomycin (100 μg/mL). The cells were inoculated to 96-well plates at a density of 5×10^4 cells/well and incubated at 37 °C with 5% (V/V) CO_2 overnight. Cells were then treated for 24 h with compounds at varying concentrations. After the removal of the medium, 100 μL of fresh medium and 10 μL of CCK-8 solution were added to each well and incubated for 3.5 h at 37 °C. A multi-detection microplate reader (BioTek Instruments Inc., VT, USA) was used to measure the absorbance at 450 nm. Cell viability was calculated as the percentage of viable cells relative to untreated cells.

The logarithmically growing RAW264.7 cells were planted onto a 96-well plate (5×10^4 cells/well) and incubated at 37 °C with 5% (V/V) CO_2. After culture for 24 h, the cells were pre-treatment with non-toxic concentrations of compounds and dexamethasone (the positive control, Shanghai Macklin Biochemical Technology Co., Ltd., Shanghai, China) for 2 h, and then were induced with lipopolysaccharide (LPS) (1 μg/mL) for another 24 h. The levels of NO, IL-6, and TNF-α in the cell supernatants was determined by ELISA assay kits (NO kit from Nanjing Jiancheng Bioengineering Institute, Nanjing, China) according to the manufacturer's instructions. All samples and the standards were performed in triplicate.

2.6 Network pharmacology-based analysis

Potential targets of compound Chro were collected from SwissTargetPrediction, SEA, and TargetNet databases. Protein targets of RA were obtained via NCBI-Gene, GeneCards, OMIM, and DisGeNET. Common targets of Chro and RA were achieved by Venny 2.1.0 platform. Protein-protein interaction (PPI) of the common targets was acquired from STRING database. Gene Ontology (GO) and Kyoto Encyclopedia of Genes and Genomes (KEGG) enrichment analysis of the crucial targets were carried out using the DAVID to obtain related functions and pathways. A "drug-targets-pathways" regulatory network was constructed by Cytoscape 3.7.0 software using PPI information and predicted pathways.

2.7 Molecular docking

The absolute configuration of compound Chro was drawn by ChemBioDraw Ultra 14.0 software, and the compound was optimized for minimum energy using Chem3D and converted to a pdb format. The crystal structures of docking proteins retrieved from the RCSB Protein Data Bank should be human derived, top-ranked by score, and at a resolution less than 2.0 Å, and saved as pdf files. Files were imported into AutoDock Tools-1.5.6 software (The Scripps Research Institute, CA, USA) and processed, and the final files were saved as pdbqt files. AutoDock Vina was used to perform semi-flexible molecular docking with the target protein set as rigid and the compound ligand structure set as flexible. The conformation search process was simulated 50 times using Lamarckian genetic algorithm. Other unmentioned conditions were maintained as defaults, and the lowest binding energy was taken as the optimal binding conformation.

2.8 Anti-RA validation in vitro

2.8.1 Cell culture

Human rheumatoid arthritis fibroblast-like synoviocytes (RA-FLS) were purchased from Saibaikang Biotechnology Co., Ltd. (Shanghai, China), and only 4−10 passages of cells were used for research. RA-FLS were cultured using high-glucose DMEM containing 10% FBS and placed in a constant temperature incubator at 37 ℃ with 5% CO_2.

2.8.2 Cell viability assay

RA-FLS growing in logarithmic phase were prepared into cell suspension at a concentration of 5×10^4 cells/mL, 100 μL was added to each well of a 96-well plate and cultured in an incubator containing 5% CO_2 at 37 ℃. After 24 h, 100 μL culture medium containing different concentrations of drugs were added to the positive group, and experimental groups, and the same amount of medium was added to the blank group (without cells) and control group (containing cells). After 24 h, 10 μL of CCK-8 reagent was added to each well, and OD was measured using a microplate reader (Bio Tek, VT, USA) after 3.5 h.

2.8.3 Migration and invasion assays

Invasion of RA-FLSs was determined with a transwell chamber with Matrigel, while migration was determined in the same way without Matrigel. RA-FLSs were inoculated in DMEM at a cell density of 3.5×10^5 cells/mL, and different concentrations of drug groups and control groups were set up. After mixing, 100 μL/well was inoculated in the upper chamber of transwell, and 600 μL medium containing 20% FBS was added to the lower chamber as the source of chemoattractant. After 24 h, the migrated cells were fixed in 4% paraformaldehyde for 1 h before staining with 0.1% crystal violet for 30 min. After washing with PBS, the unfixed cells were removed with a cotton swab. The number of cells was calculated by randomly selecting five visual fields under the light microscope.

2.8.4 Apoptosis assay

The apoptosis was analyzed by Annexin V-FITC/PI double staining kit. RA-FLSs were seeded in 6-well plates at a density of 1.0×10^5 cells/mL. After grouping, cells of the experimental groups and positive drug control group (MTX) were cultured with different concentrations of drugs and cultured at 37 ℃ and 5% CO_2. After 24 h, the cells were collected. Annexin V and Annexin-FITC were added to the cells in the dark, and the cells were incubated at 2−8 ℃ for 15 min. PI staining solution was added and incubated at 2−8 ℃ for 5 min. Then the apoptotic rate was detected by flow cytometry (Becton, Dickinson and Company, NJ, USA).

2.8.5 Cell cycle distribution assay

RA-FLSs were incubated with drugs for 24 h, and then the cells were collected and fixed by adding 70% precooled ethanol and left overnight at 4 ℃. RNase was added, followed by a water bath at 37 ℃ for 30 min. PI was added and kept in the dark for 30 min at 4 ℃. Red fluorescence was detected at a wavelength of 488 nm, and the experimental results were processed using FlowJo 10 software (Flow Cytometry Software Inc., OR, USA).

2.8.6 Detection the levels of IL-1β, IL-6, IL-8, MMP-3

RA-FLSs were pretreated with drugs for 2 h. The model group, positive group, and experimental groups were co-cultured with TNF-α (400 ng/mL) for 24 h. Then the inflammatory cytokines IL-6, MMP-3, IL-8 and IL-1β were detected by ELISA kits.

2.8.7 RNA extraction and real-time quantitative PCR (qPCR) analysis

Total RNA was isolated with TRIzol reagent. The cDNA was synthesized using a reverse transcription kit and amplified by PCR using a fluorescence quantitative kit according to the manufacturer's instruction. qPCR was performed in real-time PCR System (Roche, Basel, Switzerland) with primers as listed in Table 1.

2.8.8 Western blot analysis

After collecting the cells of each group, they were placed on ice, protein lysate was added, and the cells were vortexed and shaken every 5 min for 30 s, and repeated for 4 times to fully lyse the cells. After centrifugation (4 ℃, 12 000 r/min, 15 min), the supernatant was collected as the protein sample. Total protein was quantified using the BCA assay kit and 30 μg protein/lane was separated via SDS-PAGE. The isolated proteins were transferred onto PVDF membranes and blocked with 5% skim milk powder for 2 h.

Table 1
Primers sequences for qPCR.

Gene	Forward primer (5′-3′)	Reverse primer (5′-3′)
IL-6	CTGGTCTTTTGGAGTTTGAG	TTTCTGACCAGAAGAAGGAA
IL-8	AACTGAGAGTGATTGAGAGTGG	ATGAATTCTCAGCCCTCTTCAA
IL-1β	TTCAGGCAGGCAGTATCACTC	GAAGGTCCACGGGAAAGACAC
MMP-1	AGATTCTACATGCGCACAAATC	CCTTTGAAAAACCGGACTTCAT
MMP-3	TGAGGACACCAGCATGAACC	ACTTCGGGATGCCAGGAAAG
MMP-9	TGGACTCGGTCTTTGAGGAGC	ATAGGCTTTCTCTCGGTACTGGA
β-actin	TGGCACCCAGCACAATGAA	CTAAGTCATAGTCCGCCTAGAAGCA

Membranes were washed three times with TBST and incubated for antibodies overnight at 4 ℃ . The secondary antibodies were combined with the primary antibodies and the membranes were visualized in the automatic chemiluminescence tester by ECL and imaged using Vision Works software (UVP, CA, USA). The image gray value was calculated using ImageJ software (NIH, MD, USA).

2.9 Statistical analysis

Data presented as the mean ± standard deviation were analyzed with SPSS 19.0 (IBM, NY, USA). One-way ANOVA or *t*-test was used for analysis according to the normality and variance and other factors. Tukey multiple comparison was used as a post hoc test. $P < 0.05$ was considered statistically significant.

3. Results and discussion

3.1 Therapeutic effects of BFL on CIA rats

CIA rats were a classic animal model used for RA-related *in vivo* studies[34]. The success rate of CIA modeling is nearly 80%, and CIA rats presented a poor mental state, loss of appetite, yellowed and shedding fur, toe and ankle joint redness and swelling, and decreased activity by comparison with normal rats. After 16 days of administration, the above status of CIA rats in treatment groups was obviously improved, compared with the model group rats.

3.1.1 Effect of BFL on body weight and immune organ coefficient of CIA rats

During the observation, the body weight of normal rats showed fluctuating growth. Compared with the control, the rats body weight in model group significantly decreased from the 40th day ($P < 0.01$), while there was no significant difference in the treatment groups by comparison with the model group (Fig. 1A), suggesting BFL treatments hardly affected the body weight of CIA rats. The thymus and spleen indexes in the model group were markedly increased ($P < 0.01$), compared with the control group, and the organ indexes of medication groups (including TPT and BF-L/M/H) were significantly decreased in comparison with the model group ($P < 0.05$, Fig. 1E), indicating that BFL has a certain protective effect on immune organs of CIA rats.

3.1.2 Effect of BFL on toe swelling and arthritis score of CIA rats

On day 12, the toes of CIA rats began to swell, and reached a peak around day 20, and the swelling in right hind toe was relatively more obvious. After 20 days of medication treatment, the toe swelling in BF-L/M/H and TPT groups was significantly reduced ($P < 0.05$, Fig. 1B), compared with the model group, and the appearance and morphology of the right and left hind feet of rats were shown in Fig. 1C. The arthritis score of CIA rats was markedly high on day 24, and significantly decreased ($P < 0.01$) on the 20th day of administration (Fig. 1D), suggesting that BFL could alleviate the severity of toe redness and swelling in CIA rats.

3.1.3 Effect of BFL on ankle joint pathology of CIA rats

X-ray images showed ankle joint deformation and swelling, joint-space narrowing, roughened bone surface, and osteophyte formation in CIA rats, while BFL and TPT treatment reduced the severity of joint damage, with smoother articular surface and clearer joint space (Fig. 1G). H&E staining indicated synovial membrane hyperplasia, cartilage damage, and inflammatory cells infiltration in the model group rats, and the administration of BFL and TPT alleviated these pathological conditions a lot (Fig. 1F). Collectively, the evidence suggested BFL could effectively suppress inflammation and subsequent RA progression.

3.1.4 Effect of BFL on TNF-α, IL-6, and IL-10 levels in rat serum

Pro-inflammatory cytokines TNF-α and IL-6, and anti-inflammatory factor IL-10 were contributive to the pathogenesis of RA[35]. Serum levels of TNF-α and IL-6 were elevated in CIA rats ($P < 0.01$), while there was no significant change in IL-10 level. Twenty days after administration, the TNF-α and IL-6 levels were significantly decreased and IL-10 level ($P < 0.01$) was increased in rat serum (Figs. 1H-J), which indicated that anti-inflammation was one of the mechanisms of BFL in treating CIA.

3.2 Screening of anti-inflammatory active ingredients in BFL

The HPLC chromatogram (Fig. 2) exhibited the most abundant constituents myricetin-3-*O*-α-*L*-rhamnopyranoside (peak 1, a flavonoid

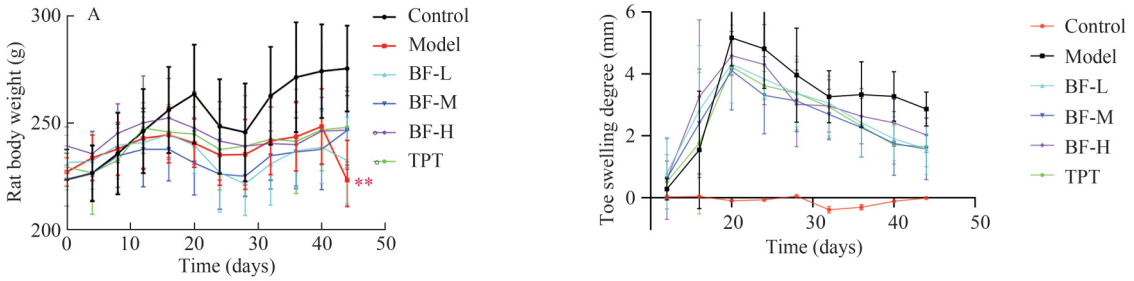


Fig. 1 Therapeutic effects of BFL on CIA rats. (A) Body weight changes. (B) Changes in toes swelling. (C) Representative morphology of ankle joints and paws. (D) Arthritis scores. (E) Thymus and spleen indexes. (F) Histopathology (H&E, arrows indicating synovial membrane hyperplasia). (G) X-ray images of right hind toes. Serum levels of (H) TNF-α, (I) IL-6, and (J) IL-10. *$P < 0.05$, and **$P < 0.01$ vs. control group; and $^{\#}P < 0.05$, and $^{\#\#}P < 0.01$ vs. model group.

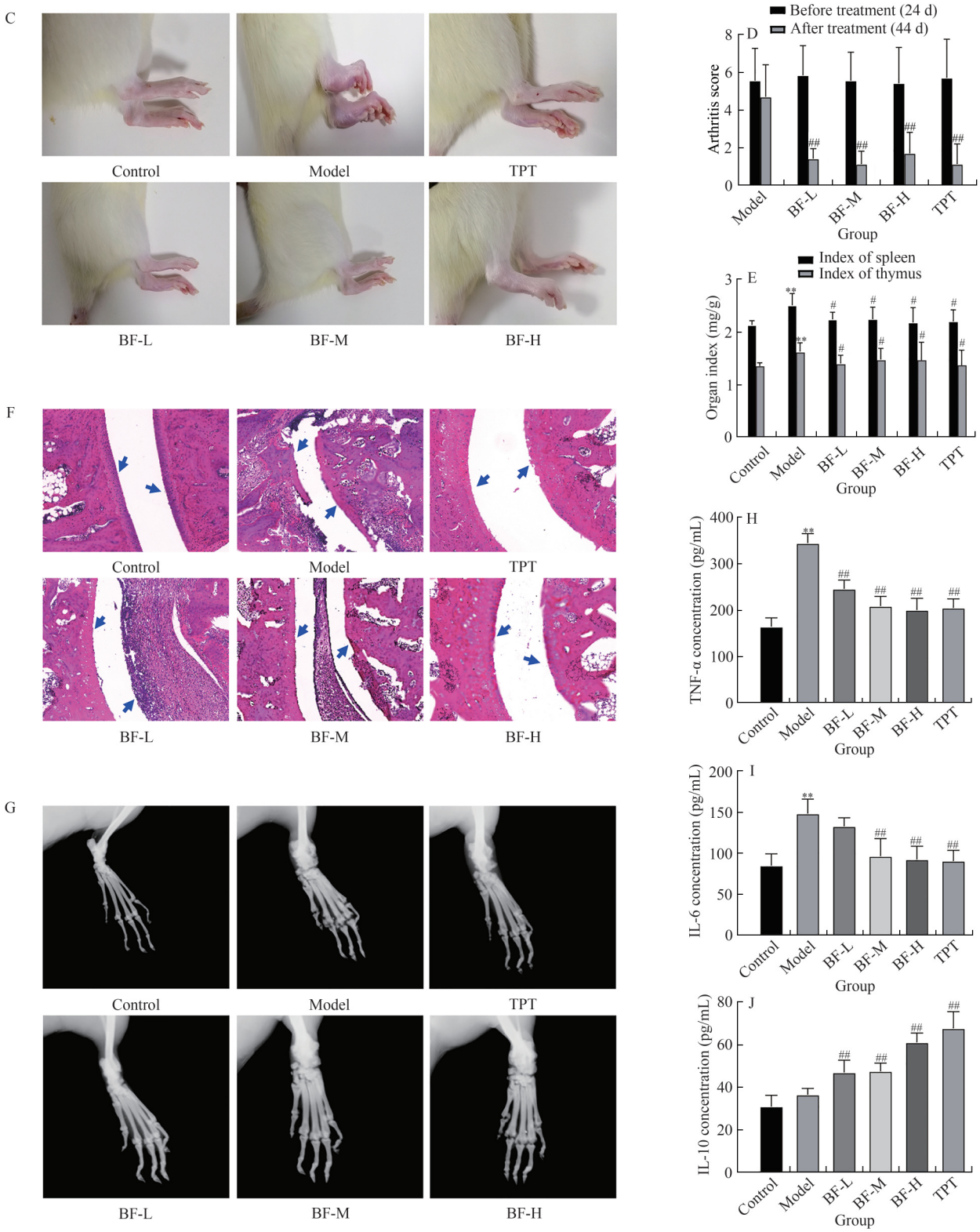


Fig. 1 (*Continued*)

compound) and Chro (peak 2, a chromone compound) in the BFL extract, with the contents of 8.4% and 9.1%, respectively. Based on LPS-induced RAW264.7 macrophages, the anti-inflammatory activities of two high-content ingredients were assayed within the non-toxic concentration range of 0−200 μg/mL, and the half maximal inhibitory concentration (IC_{50}) values indicated that compound Chro was superior to the positive drug dexamethasone in reducing the secretions of NO, IL-6, and TNF-α, suggesting potential anti-inflammatory properties (Table 2). In view of this, the predominant active constituent Chro was taken as a breakthrough to explore the anti-RA mechanism of BFL.

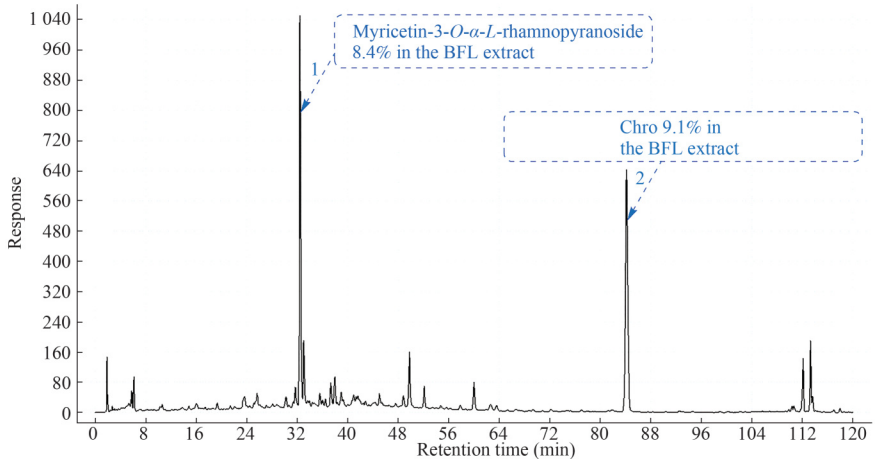


Fig. 2 HPLC analysis of BFL extract and the main active ingredients.

Table 2
Anti-inflammatory activities of main compounds in BFL.

Compounds	IC_{50} (μg/mL)		
	NO	IL-6	TNF-α
Dexamethasone	40.45 ± 1.01	> 100	> 100
Myricetin-3-*O*-α-*L*-rhamnopyranoside	> 100	> 100	> 100
Chro	41.68 ± 1.18	14.73 ± 1.30	29.66 ± 0.17

3.3 Network pharmacological analysis of Chro anti-RA

3.3.1 Targets screening of Chro against RA

The compound targets were retrieved by the name of 5-hydroxy-7-methoxy-2-isopropylchromone, and structural formulas in SMILES (CC(C)C1=CC(=O)C2=C(C=C(C=C2O1)OC)O)OC)O) and . sdf format, and 106, 45, and 156 target proteins were obtained from the databases of SwissTargetPrediction, SEA, and TargetNet, respectively. These targets with a score greater than 0.1 were merged and deduplicated, and 136 target proteins of Chro were collected. The disease targets were retrieved using "rheumatoid arthritis" as the search term, and 13 092, 3 632, and 2 722 targets were obtained from NCBI-Gene, GeneCards, and DisGeNET. The results from three database were intersected, and 1 498 human derived targets were saved as RA related targets. Finally, the above filtered targets from compound (136) and disease (1 498) were intersected, and 54 targets of compound Chro intervention in RA were achieved (Fig. 3A).

3.3.2 PPI network analysis

The PPI network for above intersecting targets was constructed (Fig. 3B), which contained 51 nodes and 185 edges (except 3 free nodes not shown), and the enrichment *P*-value was $< 1.0 \times 10^{-16}$. The color depth of each node was proportional to the degree value, and PTGS2, ESR1, CREB1, RELA (P65), IL-2, PPARG, APP, and AHR with moderately large values were more important targets for Chro acting on RA.

3.3.3 GO and KEGG analysis

The 54 intersecting targets were employed for GO functional enrichment analysis, and a total of 50 GO items (*P*-value < 0.01, false discovery rate (FDR) < 0.2) were identified. The biological process (BP, 20 terms) mainly involved positive regulation of transcription from RNA polymerase II promoter, positive regulation of transcription, DNA-templated, oxidation-reduction process, negative regulation of transcription from RNA polymerase II promoter, and xenobiotic metabolic process. The molecular function (MF, 20 terms) mainly focused on zinc ion binding, transcription factor activity, sequence-specific DNA binding, heme binding, transcription factor binding, and iron ion binding. The cell component (CC, 5 terms) was associated with nucleoplasm, axon, protein complex, organelle membrane, and histone deacetylase complex. The top 20 enriched terms of each category were shown in a histogram (Fig. 3C).

Furthermore, 30 related pathways were identified (*P*-value < 0.1, FDR < 0.4) by KEGG, and the top 20 pathways (Fig. 3D) mainly belonged to transduction-related pathway, infectious disease-related pathway, immune-system related pathway, and cancer-related pathway. Among them, the highly enriched ones such as PI3K-Akt signaling pathway, Ras signaling pathway, osteoclast differentiation, NF-κB signaling pathway, and TNF signaling pathway were closely related to the pathogenesis of RA.

The top 20 pathways and 54 key targets were introduced into Cytoscape software to construct the "compound-targets-pathway" network (Fig. 3E). Node color gradient was proportional to the degree value, and the topology analysis indicated that compound Chro mainly regulated key targets (MAPK10, RELA, RAC1, CREB1, and NOS2) via PI3K-Akt signaling pathway to play an important role in intervening RA.

These above results revealed that natural compounds acted on disease with the characteristics of multi-targets and multi-pathways. However, the predicted mechanism of action by network pharmacology with certain limitations, needed further verifications. It was

obvious that the key targets from PPI network were scattered in multiple pathways, which did not provide the main aspects (or focus) of drug acting on disease. While the KEGG analysis gave the enriched pathways, which should be preferentially chosen for mechanism validation. Comprehensive analysis of the obtained data, the PI3K-Akt pathway with the largest counts was prioritized in subsequent experiments, and then the node proteins PI3K, PDK1, AKT, and RELA, also important regulators and biomarkers, were accordingly involved.

3.4 Molecular docking analysis

Molecular docking was employed to investigate the interactions between compound Chro and key pathway proteins such as PI3K, PDK1, AKT, and RELA. All the binding energies were lower than −5.0 kcal/mol (Fig. 4), suggesting that compound Chro had good binding affinity with the 4 target proteins, and could spontaneously combine to form complexes. In terms of interaction patterns, the molecular of Chro mainly formed hydrogen bonds and hydrophobic



Fig. 3 Network pharmacological analysis of compound Chro anti-RA. (A) Venn diagram of targets of Chro and RA. (B) PPI network for key targets of Chro anti-RA. (C) Top 20 enriched GO terms in each category. (D) Bubble chart of top 20 KEGG pathways. (E) "Compound-targets-pathway" network.

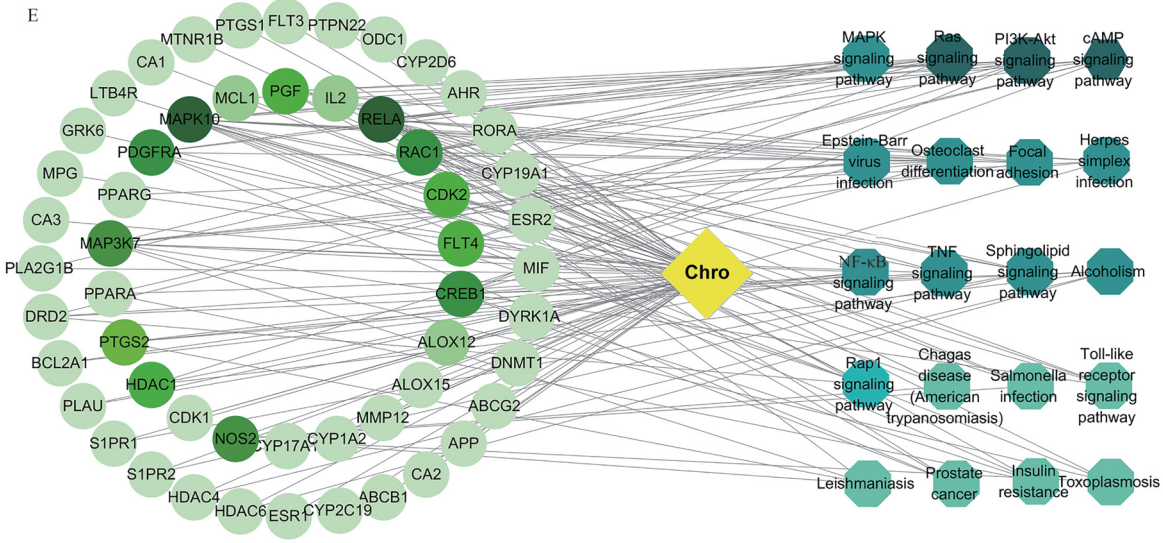


Fig. 3 (*Continued*)

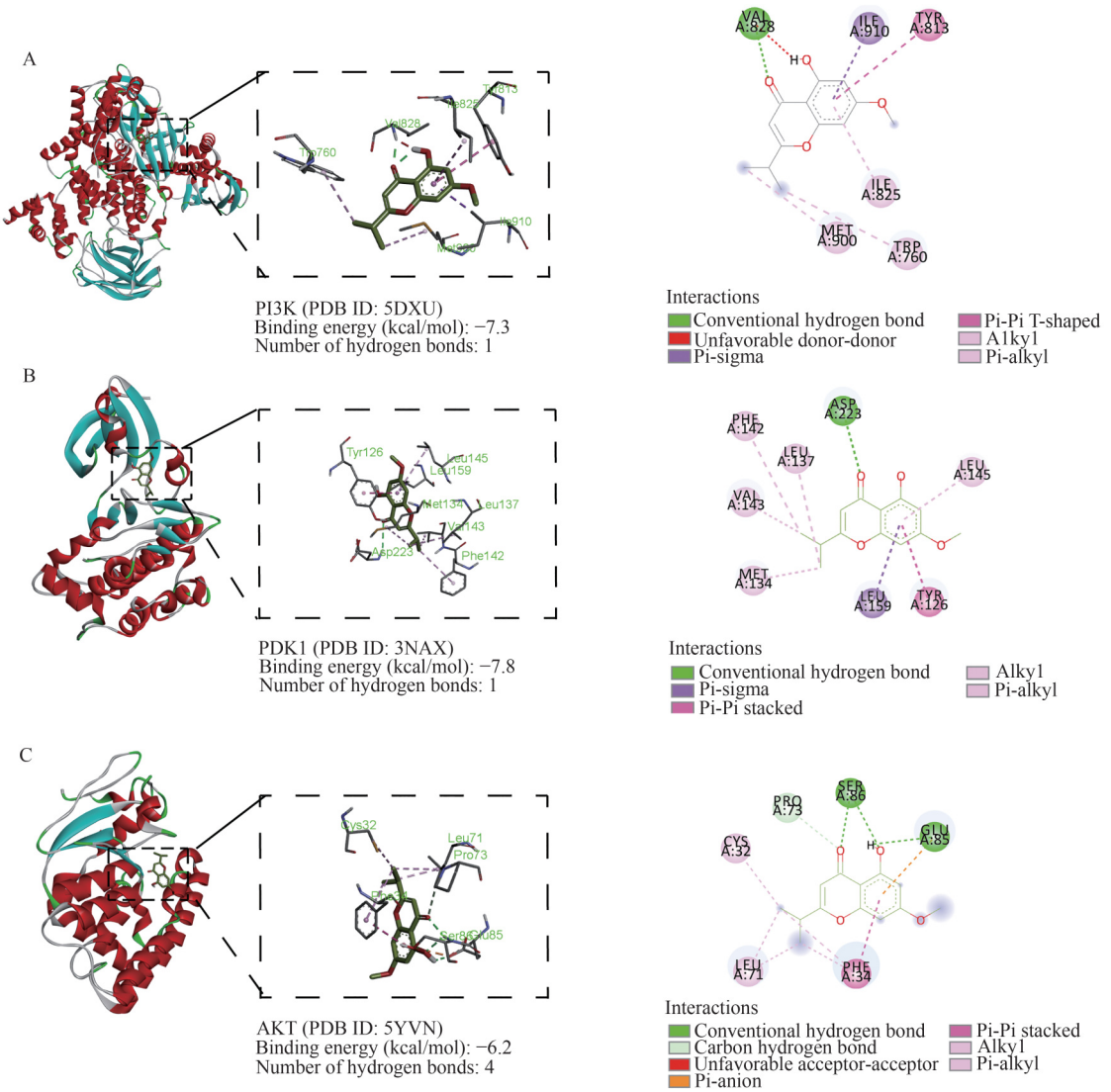


Fig. 4 Binding sites and interaction pattern of compound Chro and target proteins (A) PI3K, (B) PDK1, (C) AKT, and (D) RELA.

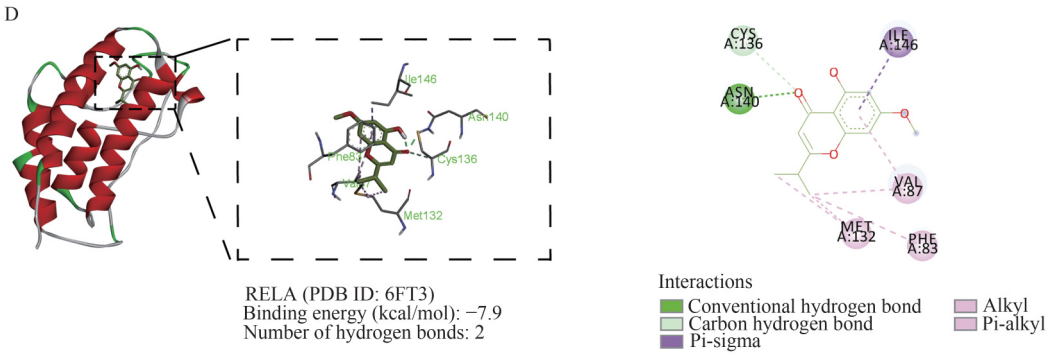


Fig. 4 (*Continued*)

interactions with corresponding amino acid residues through the 4-carbonyl, 5-hydroxyl, and 2-isopropyl groups.

3.5 *Effects and mechanism of compound Chro on RA-FLS*

3.5.1 *Chro affected the viability of RA-FLS*

RA-FLS played a pivotal role in the pathogenesis of RA[36], which was an important target cell in RA treatment, and taken as a cell model for *in vitro* validation in this research. Chro's chemical structure is shown in Fig. 5A. After 24 h of drug treatment, the viability of RA-FLS was affected in a dose-dependent manner (Fig. 5B), and the non- and low-toxic concentration ranges (cell survival rate ≥ 60%) of 0−50 μg/mL for Chro and 0−0.45 μg/mL for MTX provided basis for the concentration setting in subsequent experiments.

3.5.2 *Chro inhibited the migration and invasion of RA-FLS*

RA-FLS could migrate and invade the articular cartilage and bone, leading to destruction of cartilage and bone and joint damage[37]. In order to verify the effect of Chro on the migration and invasion ability of RA-FLS, the transwell method was used, and the data showed that compound Chro at concentrations of 25 and 45 μg/mL significantly inhibited RA-FLS migration and invasion ($P < 0.000\ 1$, Figs. 5C-F) by comparison with the bank control.

3.5.3 *Chro induced the apoptosis and cell cycle arrest in RA-FLS*

Promoting RA-FLS apoptosis was a treatment strategy for RA[38]. In this assay, compound Chro increased the cell apoptosis rate gradually with the ascending concentrations, and inhibited the over-proliferation of

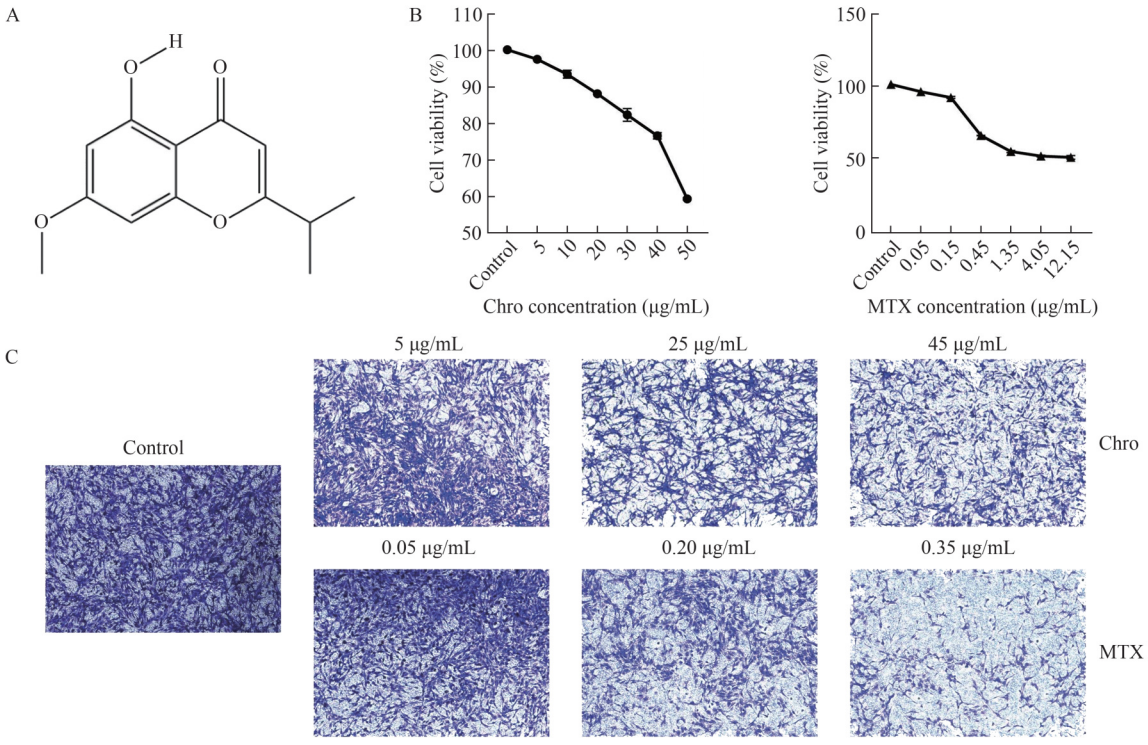


Fig. 5 Chro's chemical structure (A). Effects of compound Chro on (B) cell viability, (C and E) migration, and (D and F) invasion of RA-FLS. ***$P < 0.001$, and ****$P < 0.000\ 1$ vs. control group.

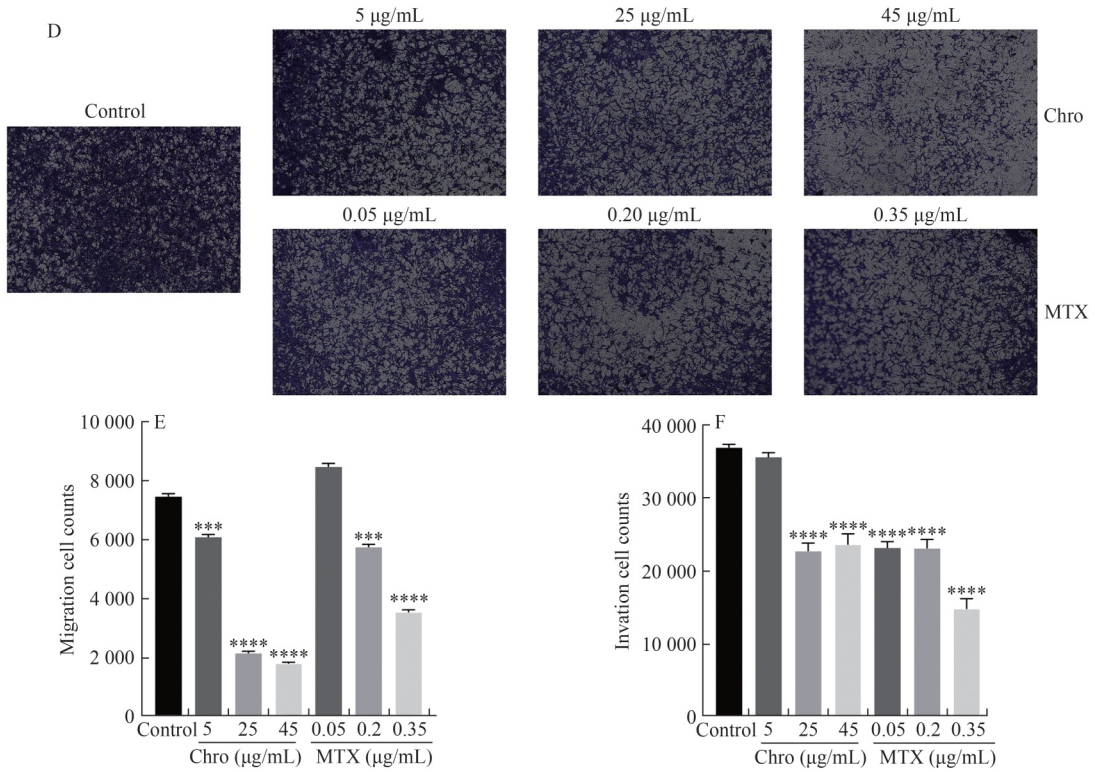


Fig. 5 (*Continued*)

RA-FLS and arrested them at G2/M phase (4N) ($P < 0.001$, Figs. 6A-B). Moreover, treatment of Chro significantly down-regulated the expressions of cell apoptosis related proteins Cyclin B1, CKD1, CDK2, Mcl-1, and Bcl-2 in RA-FLS, while up-regulated that of cleaved Caspase 3 (Fig. 6C), a characteristic protein of G2/M phase.

3.5.4 Chro inhibited the secretion of IL-6, IL-8, IL-1β, MMP-1, MMP-3, and MMP-9 in RA-FLS

RA-FLS produced various cytokines and MMPs to promote inflammation and joint destruction[39]. The TNF-α (400 ng/mL) was used to stimulate RA-FLS, and the ELISA test showed that compound Chro decreased IL-1β, IL-6, IL-8, and MMP-3 levels in cell supernatant in a concentration-dependent manner (Fig. 7A). qPCR results indicated that the mRNA expressions of *IL-1β*, *IL-6*, *IL-8*, *MMP-1*, *MMP-3*, and *MMP-9* in Chro groups were significantly reduced ($P < 0.001$, Fig. 7B) by comparison with the model group.

3.5.5 Chro inhibited the PI3K-Akt pathway in RA-FLS

Based on above network pharmacology and molecular docking analysis, the PI3K-Akt pathway was verified *in vitro*, which was a

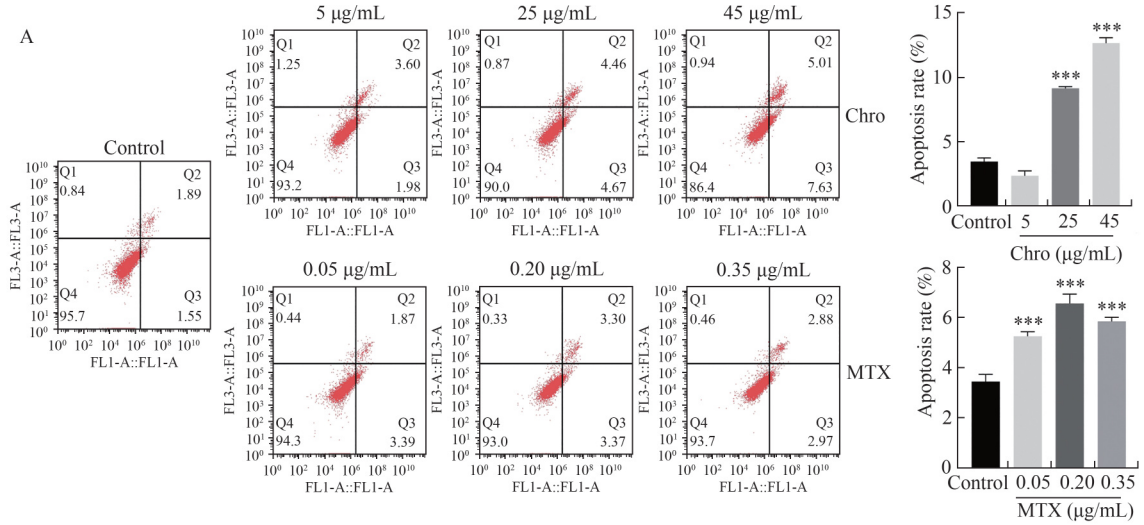


Fig. 6 Effects of compound Chro on (A) apoptosis and (B) cell cycles of RA-FLS, and (C) expressions of related marker proteins. *$P < 0.05$, **$P < 0.01$, and ***$P < 0.001$ vs. control group; $^{\#}P < 0.05$, $^{\#\#}P < 0.01$, and $^{\#\#\#}P < 0.001$ vs. model group; and ns indicates no significance ($P > 0.05$).

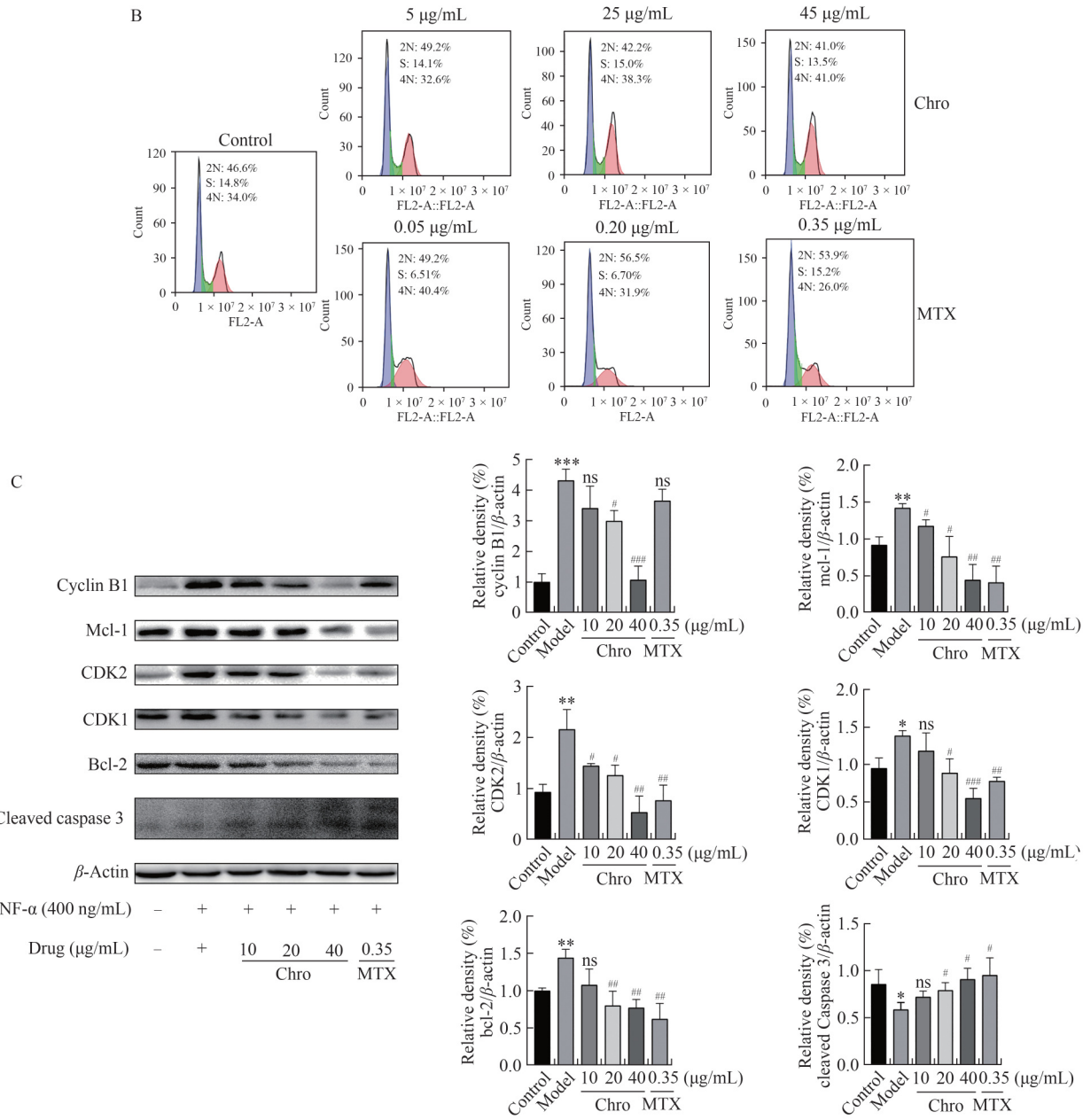


Fig. 6 (*Continued*)



Fig. 7 Effects of compound Chro on (A) secretions and mRNA expressions (B) of inflammatory cytokines in RA-FLS. $^{*}P < 0.05$, $^{**}P < 0.01$, and $^{***}P < 0.001$ vs. control group; $^{\#}P < 0.05$, $^{\#\#}P < 0.01$, and $^{\#\#\#}P < 0.001$ vs. model group; and ns indicates no significance ($P > 0.05$).

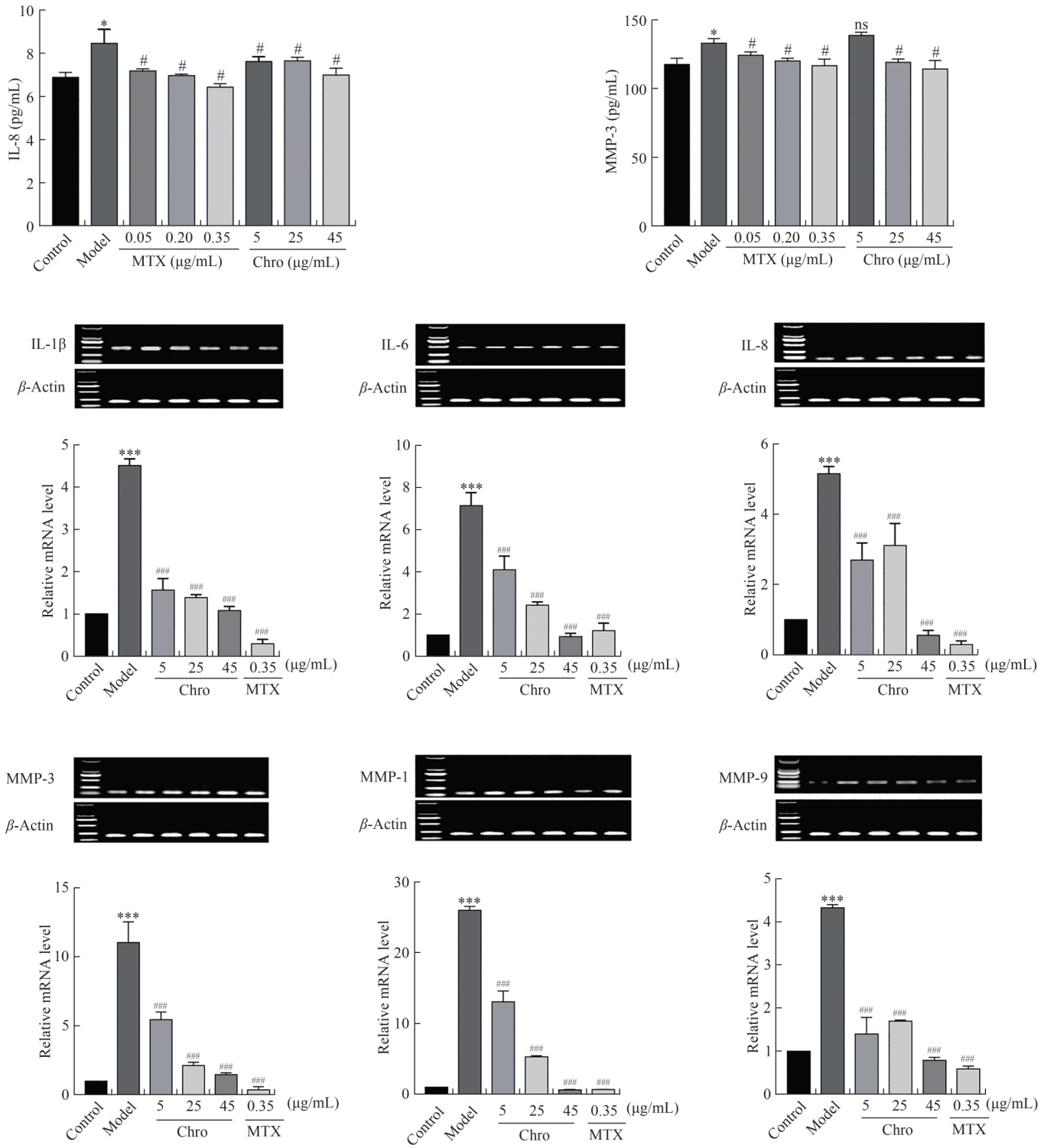


Fig. 7 (*Continued*)

potential mechanism for Chro anti-RA. The pathway node proteins were detected by Western blotting, and the results showed that Chro significantly down-regulated the expressions of PI3K, PDK1, p-Akt/Akt, and p-NF-κBp65/NF-κBp65 ($P < 0.01$, Fig. 8A).

To further evaluate the contribution of PI3K-Akt pathway in Chro treating RA, 740Y-P, a PI3K activator, was used to activate the PI3K-Akt pathway in RA-FLS. When Chro was used in combination with 740Y-P, the activation of 740Y-P on the PI3K-Akt signaling pathway was partially offset by Chro ($P < 0.01$, Fig. 8B), which suggested that compound Chro exerted interventions on RA-FLS by inhibiting the PI3K-AKT pathway.

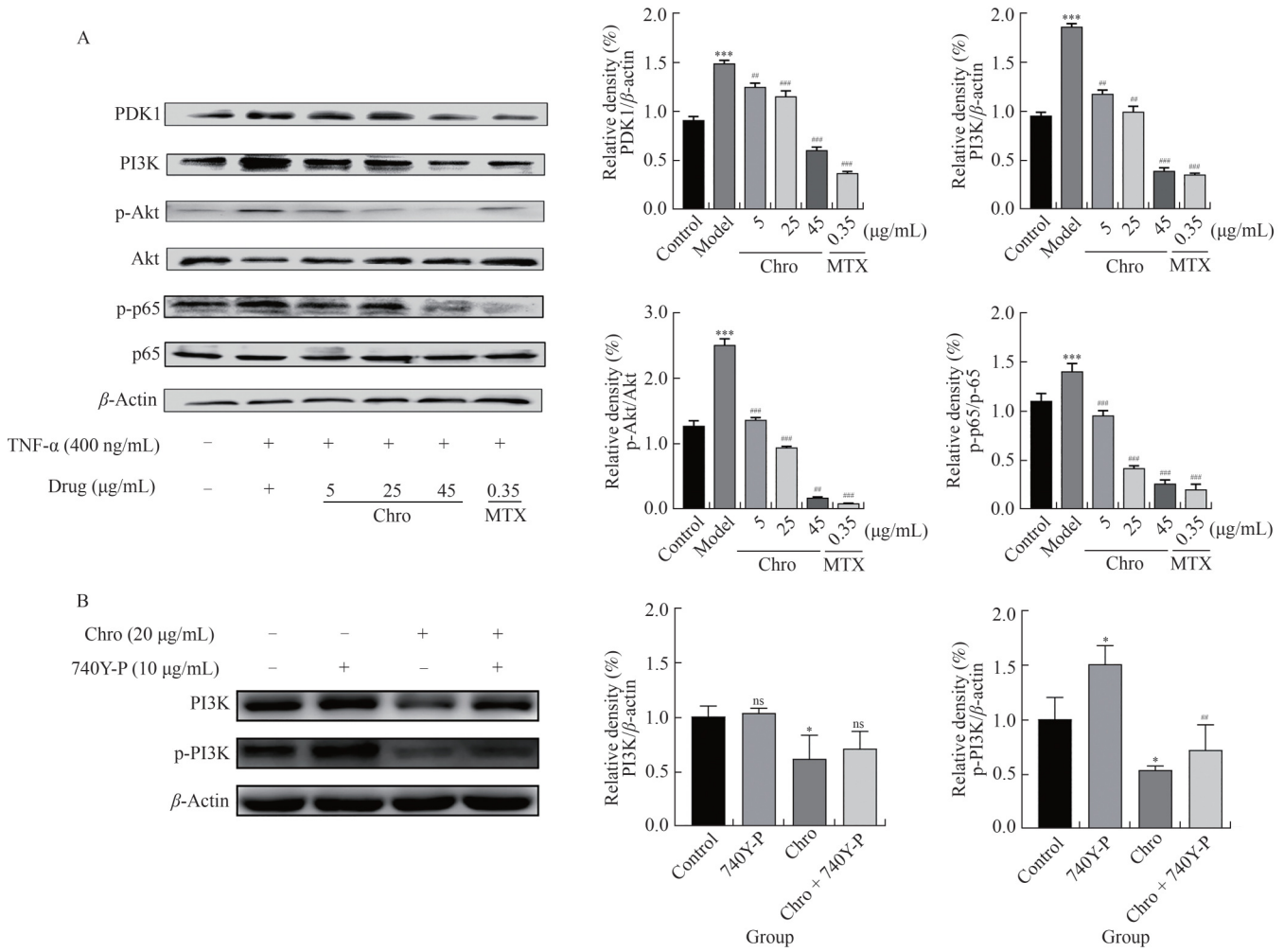


Fig. 8 Effects of compound Chro on (A) PI3K-AKT pathway in RA-FLS and (B) inhibition of PI3K activated by 740Y-P. *$P < 0.05$, and ***$P < 0.001$ vs. control group; $^{\#\#}P < 0.01$, and $^{\#\#\#}P < 0.001$ vs. model or 740Y-P group; and ns indicates no significance ($P > 0.05$).

4. Conclusion

A habit of drinking "Gang-Song-Cha" is popular throughout the South China, and the raw material BFL on anti-RA was studied in this paper. Pharmacodynamic evaluation showed that the BFL extract could ameliorate the condition of arthritis in CIA rats, but had little toxicity. Then the anti-RA mechanism of main active compound Chro was analyzed by network pharmacology and molecular docking, which suggested that the PI3K-Akt signaling pathway was a critical factor. And the cell-based experimental validation demonstrated that compound Chro could inhibit cell invasion and migration, block cell cycle and induce apoptosis, and reduce the secretion of inflammatory cytokines in RA-FLS by suppressing the PI3K-Akt pathway. All the obtained pharmacological data supported the drink (Tea) "Gang-Song-Cha" to be a functional diet, and the high-content metabolite Chro in the leaves of *B. frutescens* should be a major substance for relieving RA symptoms.

Conflict of interest

All authors declare that there are no known competing financial interests or personal relationships that could influence the work reported in this paper.

Acknowledgements

This work was supported by the National Natural Science Foundation of China (U1804182), and the Basic Research (Natural Science) Cultivation Project of Zhengzhou University (JC23852095).

Appendix A. Supplementary data

Supplementary data associated with this article can be found, in the online version, at http://doi.org/10.26599/FSHW.2024.9250166.

References

[1] A. Bean, A revision of *Baeckea* (Myrtaceae) in eastern Australia, Malesia and south-east Asia, Telopea 7(3) (1997) 245-260. https://doi.org/10.7751/telopea19971018.

[2] N.S. Ahmad, M.N.A. Ghani, A.M. Ali, et al., High performance liquid chromatography (HPLC) profiling analysis and bioactivity of *Baeckea frutescens* L. (Myrtaceae), J. Plant Stud. 1(2) (2012) 101-108. https://doi.org/10.5539/jps.v1n2p101.

[3] N.T. Tam, D.T. Thuam, A. Bighelli, et al., *Baeckea frutescens* leaf oil from Vietnam: composition and chemical variability, Flavour Fragrance J. 19(3) (2004) 217-220. https://doi.org/10.1002/ffj.1281.

[4] B.M. Liu, M.X. Lai, K.N. Liang, et al., Study on quality analysis of essential oil from twig and leaf of *Baeckea frutescens*, China J. Chin. Mater. Med. 29(6) (2004) 539-542. https://doi.org/10.3321/j.issn:1001-5302.2004.06.015.

[5] Y. Fujimoto, S. Usui, M. Makino, et al., Phloroglucinols from *Baeckea frutescens*, Phytochemistry 41(3) (1996) 923-925. https://doi. org/10.1016/0031-9422(95)00659-1.

[6] K. Nisa, T. Ito, T. Kodama, et al., New cytotoxic phloroglucinols, baeckenones D-F, from the leaves of Indonesian *Baeckea frutescens*, Fitoterapia 109 (2016) 236-240. https://doi.org/10.1016/j.fitote.2016.01.013.

[7] T. Ito, K. Nisa, S.K. Rakainsa, et al., New phloroglucinol derivatives from Indonesian *Baeckea frutescens*, Tetrahedron 73(8) (2017) 1177-1181. https://doi.org/10.1016/j.tet.2017.01.016.

[8] W.Y. Tsui, G.D. Brown. Chromones and chromanones from *Baeckea frutescens*, Phytochemistry 43(4) (1996) 871-876. https://doi.org/10.1016/0031-9422(96)00360-3.

[9] C.A. Gray, P.T. Kaye, A.T. Nchinda. Chromone studies. part 13.[1] synthesis and electron-impact mass spectrometric studies of 5-hydroxy-2-isopropyl-7-methoxychromone, a constituent of the medicinal plant *Baeckea frutescens*, and side-chain analogue, J. Nat. Prod. 66(8) (2003) 1144-1146. https://doi.org/10.1021/np030097d.

[10] B.X. Jia, X.L. Zeng, F.X. Ren, et al., Baeckeins F-I, four novel C-methylated biflavonoids from the roots of *Baeckea frutescens* and their anti-inflammatory activities, Food Chem. 155 (2014) 31-37. https://doi.org/10.1016/j.foodchem.2014.01.022.

[11] J. N. Zhou, M. Yan, P. Gao, et al., New flavonoids and methylchromone isolated from the aerial parts of *Baeckea frutescens* and their inhibitory activities against cyclooxygenases-1 and -2, Chin. J. Nat. Med. 16(8) (2018) 615-620. https://doi.org/10.1016/S1875-5364(18)30099-2.

[12] C.J. Jia, X.M. Sun, X.Y. Zhang, et al., Baeckeins L M, two novel C-methylated triflavonoids from the roots of *Baeckea frutescens* L., Nat. Prod. Res. 34(2) (2020) 278-283. https://doi.org/10.1080/14786419.2018.1528590.

[13] B.X. Jia, F.X. Ren, L. Jia, et al., Baeckein E, a new bioactive C-methylated biflavonoid from the roots of *Baeckea frutescens*, Nat. Prod. Res. 27(22) (2013) 2069-2075. https://doi.org/10.1080/14786419.2013.778852.

[14] S. Razmavar, M.A. Abdulla, S.B. Ismail, et al., Antibacterial activity of leaf extracts of *Baeckea frutescens* against methicillin-resistant *Staphylococcus aureus*, Biomed. Res. Int. 2014 (2014) 521287. https://doi.org/10.1155/2014/521287.

[15] T.T. Vu, H. Kim, V.K. Tran, et al., *In vitro* antibacterial activity of selected medicinal plants traditionally used in Vietnam against human pathogenic bacteria, BMC Complement. Altern. Med. 16 (2016) 32. https://doi.org/10.1186/s12906-016-1007-2.

[16] H. Jiang, M. Zhang, L. Qin, et al., Chemical composition of a supercritical fluid (Sfe-CO2) extract from *Baeckea frutescens* L. leaves and its bioactivity against two pathogenic fungi isolated from the tea plant (*Camellia sinensis* (L.) O. Kuntze), Plants 9(9) (2020) 1119. https://doi.org/10.3390/plants9091119.

[17] J.Q. Hou, C. Guo, J.J. Zhao, et al., Anti-inflammatory meroterpenoids from *Baeckea frutescens*, J. Nat. Prod. 80(8) (2017) 2204-2214. https://doi.org/10.1021/acs.jnatprod.7b00042.

[18] Q.W. Yu, H. Wang, J.T. Huo, et al., Suppression of *Baeckea frutescens* L. and its components on MyD88-dependent NF-κB pathway in MALP-2-stimulated RAW264.7 cells, J. Ethnopharmacol. 207 (2017) 92-99. https://doi.org/10.1016/j.jep.2017.05.034.

[19] X. Lin, J. Zhang, D. Fan, et al., Frutescone O from *Baeckea frutescens* blocked TLR4-mediated Myd88/NF-κB and MAPK signaling pathways in LPS induced RAW264.7 macrophages, Front. Pharmacol. 12 (2021) 643188. https://doi.org/10.3389/fphar.2021.643188.

[20] X. Lin, H. Wang, X. An, et al., Baeckein E suppressed NLRP3 inflammasome activation through inhibiting both the priming and assembly procedure: implications for gout therapy, Phytomedicine 84 (2021) 153521. https://doi.org/10.1016/j.phymed.2021.153521.

[21] T. Ito, K. Nisa, T. Kodama, et al., Two new cyclopentenones and a new furanone from *Baeckea frutescens* and their cytotoxicities, Fitoterapia 112 (2016) 132-135. https://doi.org/10.1016/j.fitote.2016.05.017.

[22] S.H. Shahruzaman, M.F. Mustafa , S. Ramli, et al., The cytotoxic properties of *Baeckea frutescens* branches extracts in eliminating breast cancer cells, Evid. Based Complement. Alternat. Med. 2019 (2019) 9607590. https://doi.org/10.1155/2019/9607590.

[23] S. Navanesan, N. A. Wahab, S. Manickam, et al., Evaluation of selected biological capacities of Baeckea frutescens, BMC Complement. Altern. Med. 15 (2015) 186. https://doi.org/10.1186/s12906-015-0712-6.

[24] Y.J. Li, X.F. Chen, Z.X. Zhong, et al., Experimental study on pharmacological effects of alcohol extract of *Baeckea fruiescents* L., ZhongGuo ZhongYiYao KeJi 16(3) (2009) 192-194.

[25] Y.J. Li, X.F. Chen, Z.X. Zhong, et al., Experimental study on pharmacological effects of aqueous extract of *Baeckea fruiescents* L., Journal of Chinese Medicinal Materials 11 (2007) 1429-1432. https://doi.org/10.13863/j.issn1001-4454.2007.11.029.

[26] J.U. Scher, S.B. Abramson, The microbiome and rheumatoid arthritis, Nat. Rev. Rheumatol. 7(10) (2011) 569-578. https://doi.org/10.1038/nrrheum.2011.121.

[27] M.R. Ben, N. Bouchmaa, H. Ainani, et al., Anti-rheumatoid drugs advancements: new insights into the molecular treatment of rheumatoid arthritis, Biomed. Pharmacother. 151 (2022) 113126. https://doi.org/10.1016/j.biopha.2022.113126.

[28] X. Liu, Z. Wang, H. Qian, et al., Natural medicines of targeted rheumatoid arthritis and its action mechanism, Front. Immunol. 13 (2022) 945129. https://doi.org/10.3389/fimmu.2022.945129.

[29] H. Sun, Y. Guo, H. Wang, et al., Gut commensal *Parabacteroides distasonis* alleviates inflammatory arthritis, Gut 72(9) (2023) 1664-1677. https://doi.org/10.1136/gutjnl-2022-327756.

[30] K.D. Moudgil, S.H. Venkatesha, The anti-inflammatory and immunomodulatory activities of natural products to control autoimmune inflammation, Int. J. Mol. Sci. 24(1) (2022) 95. https://doi.org/10.3390/ijms24010095.

[31] X.B. Lin, H. Wang, J.H. Zhang, et al., Screening of prostaglandin E2 receptor 4 antagonist from active compounds of *Baeckea frutescens* L. and its anti-rheumatoid arthritis effect *in vivo*, Journal of China Pharmaceutical University 52(1) (2021) 92-99.

[32] S. Lucas, Y. Omata, J. Hofmann, et al., Short-chain fatty acids regulate systemic bone mass and protect from pathological bone loss, Nat. Commun. 9(1) (2018) 55. https://doi.org/10.1038/s41467-017-02490-4.

[33] B.X.Jia, Q.Q. Huangfu, F.X. Ren, et al., Identification and quantification of flavonoids and chromes in *Baeckea frutescens* by using HPLC coupled with diode-array detection and quadruple time-of-flight mass spectrometry, Nat. Prod. Res. 29(9) (2015) 800-806. https://doi.org/10.1080/14786419.2014.987144.

[34] C. Zhao, X. Li, Y. Yang, et al., An analysis of Treg/Th17 cells imbalance associated microRNA networks regulated by moxibustion therapy on Zusanli (ST36) and Shenshu (BL23) in mice with collagen induced arthritis, Am. J. Transl. Res. 11(7) (2019) 4029-4045. https://www.ncbi.nlm.nih.gov/pmc/articles/PMC6684903/.

[35] M. Kirchmeyer, M. Koufany, S. Sebillaud, et al., All-trans retinoic acid suppresses interleukin-6 expression in interleukin-1-stimulated synovial fibroblasts by inhibition of ERK1/2 pathway independently of RAR activation, Arthritis Res. Ther. 10(6) (2018) R141. https://doi.org/10.1186/ar2569.

[36] G. Nygaard, G.S. Firestein. Restoring synovial homeostasis in rheumatoid arthritis by targeting fibroblast-like synoviocytes, Nat. Rev. Rheumatol. 16 (6) (2020) 316-333. https://doi.org/10.1038/s41584-020-0413-5.

[37] W. Zhou, Q. Shen, H. Wang, et al., Knockdown of YAP/TAZ Inhibits the migration and invasion of fibroblast synovial cells in rheumatoid arthritis by regulating autophagy, J. Immunol. Res. 2020 (2020) 9510594. https://doi.org/10.1155/2020/9510594.

[38] L.M. Zhang, J.J. Zhou, C. L. Luo, CYLD suppression enhances the pro-inflammatory effects and hyperproliferation of rheumatoid arthritis fibroblast-like synoviocytes by enhancing NF-κB activation, Arthritis Res. Ther. 20(1) (2018) 219. https://doi.org/10.1186/s13075-018-1722-9.

[39] Y. Tang, B. Wang, X. Sun, et al., Rheumatoid arthritis fibroblast-like synoviocytes co-cultured with PBMC increased peripheral $CD4^{+}CXCR5^{+}ICOS^{+}$T cell numbers, Clin. Exp. Immunol. 190(3) (2017) 384-393. https://doi.org/10.1111/cei.13025.